



Analysis of Continuous Motion Angle for Lower Limb Exoskeleton Robot Based on sEMG Signal

Liuwen Jing^(✉), Tie Liu, Haoming Shi, Yinming Shi, Shiyu Yao, Junyou Yang, Xia Yang, and Dianchun Bai

Shenyang University of Technology, No. 111, Shenyang Economic and Technological Development Zone, Shenyang, Liaoning, China
ytnmjingliuwen@163.com

Abstract. In this paper, the state of real-time motion angle corresponding to the surface electromyography signal (sEMG) in the process of exoskeleton robot assisted motion is analyzed, and a new control analysis method for exoskeleton robot is proposed. The method of wavelet decomposition is used to analyze the characteristics of sEMG signals, which can accurately extract the eigenvalues of sEMG signals from different angles. The extracted eigenvalues are used as the input of SVM classification and recognition, pattern recognition is carried out, and the relationship between the eigenvalues and the corresponding motion angle is established. At the same time, the surface EMG signals of the start and stop time in the process of continuous movement of the lower limbs are analyzed to obtain a more accurate relationship between the start and stop state and the eigenvalue. By comparing the analysis results with the actual movement angle state information, the correctness of the analysis results is verified, which provides a theoretical basis for the follow-up research of the lower extremity exoskeleton robot.

Keywords: sEMG signal · Continuous movement of lower limbs · Lower limb exoskeleton robot · Wavelet feature extraction · SVM support vector machine

1 Introduction

With the development of national economy, science and technology, and the improvement of people's living standards, promoting and improving the medical welfare of disabled people has become a very concerned issue of the government. As a representative human-computer interaction robot, wearable human exoskeleton robot has been highly valued in military, civil and rehabilitation treatment. Among them, the wearable exoskeleton robot applied to the lower limbs of human body can enhance the movement ability of the lower limbs under the control of the wearer. Exoskeleton mechanical system further calculates and controls the output in real time by estimating and predicting the motion state and intention of human body, so as to realize real-time and synchronous strength enhancement and assistance, enhance human body function, and enable human body to complete many tasks with the help of machinery [1].

Historically, the typical system is a series of exoskeletons built by m.vukobratovic and others. They have developed different types of exoskeletons, powered by hydraulic actuators, pneumatic actuators and DC servo motors, and verified the theoretical results. However, the control system is relatively backward, which can not achieve the precise and free control of the user exoskeleton robot [2]. At present, most mature Rehabilitation Exoskeleton robots are developed by foreign companies or institutions. For example, Hal exoskeleton robot developed by the University of Tsukuba in Japan can help the elderly and the disabled walk; eLeg exoskeleton system of belike bionics company in the United States can help paraplegic patients completely get rid of wheelchairs to walk independently, and can also help people who can't stand to train lower limb muscles and nerves. The research of domestic and foreign skeleton robots is mainly concentrated in universities and research institutes. Yang Canjun's team of Zhejiang University has developed a prototype of lower limb exoskeleton with pneumatic actuator, which uses the adaptive fuzzy artificial neural network algorithm to input the pressure sensor data of the wearer's sole, calculate the expected action of the exoskeleton robot, and drive the lower limb hip joint and knee joint. Realize the control of exoskeleton robot [3]. Harbin University of technology designed the lower limb dynamic exoskeleton machine to control through the sensing data and the robot's motion position. Gait prediction is realized by the pressure sensor placed on the sole of the foot. However, the collection of foot pressure information often lags behind the actual action of the user, which leads to the action delay of the exoskeleton robot [4]. A wearable lower limb exoskeleton developed by the Chinese Academy of Sciences, which drives the hip and knee joints, is controlled by predefined trajectory, input the joint angle of normal people, and reproduce it on the exoskeleton. But the predefined orbit is often difficult to meet the user's movement diversity in actual use. Most of them mainly study the assisted exoskeleton robot, but few research the Rehabilitation Exoskeleton Robot. In addition, the research and development of the rehabilitation exoskeleton is still in the primary stage, most of which are treadmill type structures. The patients are passively trained after wearing the equipment, which is a certain distance from the practical application and active training [5]. Although the existing identification methods have achieved good results, there are still many problems. Most of the studies are less concerned with feature selection and usually adopt some combination of features directly. If these features are directly applied to gait recognition, the classification effect is poor. The present algorithm has poor performance in real-time control and long response time. In order to solve the problems existing in the above methods, a new algorithm for the continuous motion state of lower extremity exoskeleton robot based on surface emG signal is proposed in this paper, and continuous kick motion is taken as an example for analysis and verification. Type of rehabilitation of exoskeleton robot research and electromyographic signal analysis of lower limb movement condition, can get lower limb under different angles in the process of movement of electrical information, using the MATLAB data simulation verify its rationality at the same time, and get the reasonable motor driven data, for subsequent the electromyographic signal data analysis as well as the mechanical structure and drive system and design to provide the reference [6–10].

2 Experiment

2.1 Subjects

20 healthy volunteers were recruited, including 12 male volunteers and 8 female volunteers. There was no sports injury within 7 days before the experiment. There were no motor nerve diseases, no sprains, sports injuries, fractures and other injuries affecting the motor function in the lower limbs before the experiment; no strenuous exercise in the two days before the experiment; no muscle soreness and discomfort. The subjects were between 22 and 26 years old, with an average age of 24.7 (± 1.08) years, height of 174.1 (± 3.72) cm, and weight of 68.6 (± 7.26) kg. In the definite experiment Start the experiment after the content [11].

2.2 Experiment Process

The equipment used in this experiment includes: electromyographic sensor, Tektronix oscilloscope, AgCl electrode, WSSS motion sensing system, etc. [12]. The target muscles detected in the experiment are the outer, rectus, inner and semitendinosus muscles of the lower limbs of normal human body. Before the experiment, the skin of the experimenter was wiped with a scrub and medical alcohol to reduce the influence of skin impedance on the experimental results.

The surface electrode was pasted on the abdomen of the outer thigh [13], rectus femoris, inner thigh and semitendinosus muscles, and the direction of the surface electrode was parallel to the longitudinal axis of the muscle fiber as far as possible; WSSS motion sensor was pasted on the skin surface of the midline of the outer thigh of the subject, and the height of the motion sensor was consistent with the height of the fingertip when the hands were released and lowered, and the y-axis direction of the sensor was kept at 0° . In order to reduce the artificial error of the experiment, the subjects are required to adopt the same standing posture, feet together, hands naturally drooping and relaxing. During the experiment, the subjects swung naturally with one leg according to the requirements, and set the position of standing with both legs together as the initial position. According to the requirements, the subjects began to swing forward from the initial position to the highest point of natural swing, and then changed to swing backward. After the initial position, they continued to swing backward to the highest point of natural swing, and changed to swing forward to the initial position [14]. The whole process is continuous and each group of actions is repeated five times. The action time of each group should not be less than 6 s, and the rest should be at least 30 s at the end of every five groups of actions, so as to prevent muscle fatigue from affecting the authenticity of experimental data. The specific experimental process is shown in Fig. 1.

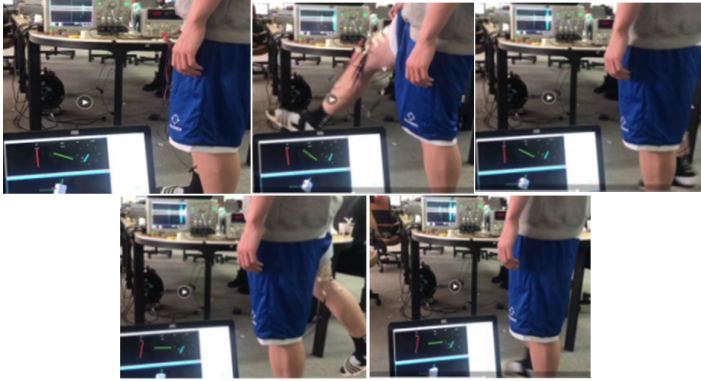


Fig. 1. The experimental schematic.

3 Data Analysis and Experimental Results

3.1 Analysis of Starting and Stopping Points of Movement

The collected sEMG signal and movement angle data are input into the computer, and the simulation experiment is carried out by using MATLAB [15–17]. According to the corresponding relationship of the time information of sEMG signal in the movement angle data, the starting point of each group of actions is determined, and the sEMG signal located in the position interval between the starting point and the ending point of each group of actions is recorded, which is used for the four movement stages of each group of sEMG signals divide. According to the movement angle data and time, the collected EMG signals of each group of continuous movement are divided into four segments, which are: the initial position moves to the front highest point, the front highest point to the initial position, the initial position to the back highest point and the back highest point to the original position. In order to ensure the accuracy of the follow-up analysis, the synchronization of the angle data and the surface EMG signal data is realized to the greatest extent, and the accurate starting and stopping points of each action part are obtained. Figure 2 shows the complete angle data of five groups of actions in an experiment. According to the data initial value, maximum value and minimum value, the starting point and stopping point of a group of actions can be analyzed, and then the exact time corresponding to the starting point and stopping point can be obtained according to the corresponding relationship between the time measured by the Angle sensor and the Angle. Figure 3 shows the raw EMG data of a complete experiment. By comparing the time data of EMG data, the corresponding starting and stopping points of emg signals were found, so that the complete five consecutive EMG signals obtained in the experiment were decomposed into the motion of a single group of continuous emg signals. Figure 4 shows the continuous EMG signal after the extraction of the active segment [18].

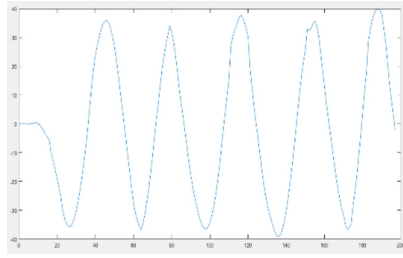


Fig. 2. Movement angle data of one group of subjects

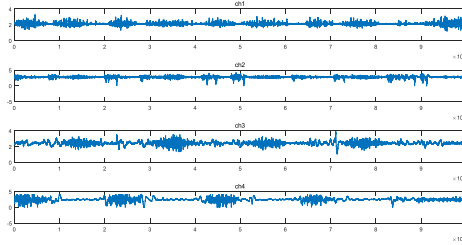


Fig. 3. Original sEMG signal.

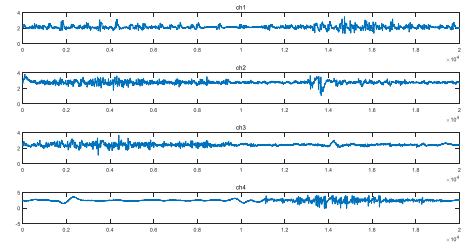


Fig. 4. Continuous sEMG signal after active segment extraction.

3.2 Analysis of Starting and Stopping Points of Movement

Wavelet transform (WT) is a time-frequency analysis method which has the same window size (area) but variable window shape, time window and frequency window. Wavelet transform has lower time resolution and higher frequency resolution in the application of low-frequency signals, but higher time resolution and lower frequency resolution in the analysis of high-frequency signals, which makes wavelet transform have good adaptability in the analysis of different sEMG signals [19].

The essence of wavelet analysis method is to decompose the signal $s(t)$ into sub signals in different frequency bands of the basis function, and analyze the changes of surface EMG signal in the process of muscle dynamic contraction from the perspective of frequency domain. Wavelet has the characteristics of multi-resolution [20], which can gradually observe the signal from coarse to fine. Wavelet transform can be

understood as a function of scale factor a and translation factor b . in the process of wavelet transform, changing the value of b only affects the position of the window on the time axis, while scale a not only affects the position of the window on the frequency axis, but also affects the shape of the window [21].

The continuous wavelet transform of the input signal of basic wavelet or parent wavelet is defined as the function family $\psi(a, b)$ generated by scale factor a and translation factor b :

$$\psi_{a,b}(t) = \frac{1}{\sqrt{a}} \psi\left(\frac{t-b}{a}\right) \quad a, b \in \mathbb{R}, a \neq 0 \quad (1)$$

It is called analytical wavelet or continuous wavelet (CWT). The coefficients in the formula are used to realize the normalization of energy in the expansion process. The definition of continuous wavelet transform of $s(t)$ is as follows:

$$W_s(a, b) = \int_{-\infty}^{+\infty} s(t) \psi_{a,b}^*(t) dt \quad (2)$$

Figure 5 is a comparison between the original surface EMG signal of four muscles in five groups of exercise and the signal after noise reduction by two methods.

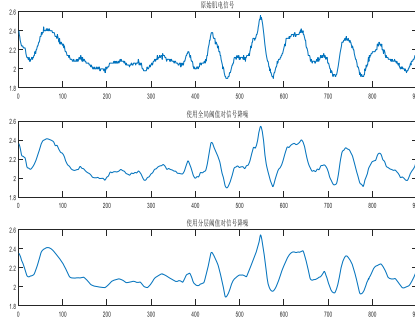


Fig. 5. Surface electromyography of a subject after noise reduction during continuous exercise

Through the method of unbiased likelihood estimation based on Stein, the noise reduction command is used to complete the signal noise reduction. There are two ways to select the threshold: global threshold and layered threshold. The global threshold applies the SURE principle, and the layered threshold applies and displays its advantages through data. From Fig. 5, it can be seen that the signal denoised by the global threshold and layered threshold method retains the high-frequency characteristics of the signal well. Between the two, the layered threshold loses the performance of the signal (compared with the original signal) Compared with the global threshold, the layered threshold reduces the details of the signal and loses some information.

3.3 Feature Extraction

The main purpose of the feature extraction module is to obtain the relationship between the muscle signals and time-frequency domain features during arm movement [22].

In order to ensure the real-time performance of the system, while ensuring the accuracy, the time-frequency domain feature with small amount of computation and rapid acquisition is used as the information measure.

In this paper, the method of wavelet analysis is used to decompose surface emg signals into low-frequency and high-frequency components. After several transformations, the data volume and frequency of each transformation are halved, and the multi-resolution decomposition of the original signal is finally realized.

In the process of wavelet decomposition, let the total frequency band occupied by the original emg signal $f(t)$ be the space V_0 . After the first stage decomposition, V_0 is divided into the scale signal space V_1 of low frequency and the wavelet signal space W_1 of high frequency. Therefore, V_1 and W_1 are the subspaces of V_0 and can be expressed as $V_1 \oplus W_1 = V_0$. In order to decompose downward, multiple spatial decomposition can be obtained, that is, the multi-resolution analysis of wavelet.

When the low-frequency scale signal and the high-frequency wavelet signal are used to reconstruct the emg signal, it can be seen that the low-frequency signal component is relatively rough, while the high-frequency signal is relatively fine, so it can effectively represent the different components of the signal, which is conducive to the signal analysis and processing. In the orthogonal wavelet analysis, the scale function V_j and the wavelet function W_j have the same importance. The scale equation of the scale function $\varphi(t)$ is established through the multi-resolution analysis, and then the wavelet function $\psi(t)$ is obtained. Then the multi-resolution wavelet transform equation of function $g(t)$ is as follows:

$$g(t) = \sum_{k=-\infty}^{\infty} c(k)\varphi_k(t) + \sum_{j=0}^{\infty} \sum_{k=-\infty}^{\infty} d(j,k)\psi_{j,k}(t) \quad (3)$$

The scale coefficient and wavelet coefficient are expressed as

$$c_{j,k} = \langle g(t), \varphi_{j,k}(t) \rangle \quad (4)$$

$$d_{j,k} = \langle g(t), \psi_{j,k}(t) \rangle \quad (5)$$

Therefore, the surface emg signal is decomposed through the wavelet coefficients of different scales. The wavelet coefficients of each level are taken as the characteristics of the signal, and the signal can be accurately described by a few coefficients. Due to the non-stationarity of surface emg signals, it is important to choose a suitable wavelet base for the effective classification and recognition of signals. Symlets wavelet function system is an approximate symmetric wavelet function, which is an improvement on db function. The Symlets system of functions is usually represented as symN ($N = 2, 3, \dots, 8$). The support range of symN wavelet is $2N - 1$, the vanishing moment is N , and it also has good normality. Compared with dbN wavelet, this wavelet is consistent with dbN wavelet in terms of continuity, support length, filter length, etc., but symN wavelet can reduce phase distortion during signal analysis and reconstruction

to some extent. In this paper, the well-classified orthogonal Sym3 wavelet basis function is selected to decompose the emg signal at five scales, and the singular value and energy value of each wavelet coefficient are extracted as the eigenvectors.

After preprocessing the sEMG signals collected by the four motion modes of the legs, the feature scatter diagram distribution after feature extraction by wavelet decomposition method is shown in Fig. 6.

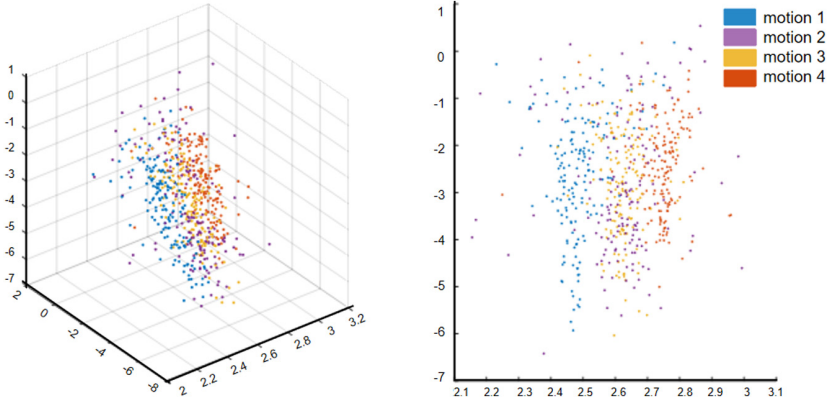


Fig. 6. Spatial distribution scatter of four kinds of action eigenvalues.

It can be seen from the feature scatter diagram that the feature values of different actions have a very light clustering effect, which can realize the feature representation of the four action modes and satisfy the desired pattern recognition rate.

4 Classification and Recognition

The method of support vector machines (SVM) is based on statistical learning theory. Suppose that the selected linear separable sample set is [23]:

$$(x_i, y_i) (i = 1, 2, \dots, N, x_i \in R^n, y \in \{-1, 1\}) \quad (6)$$

According to the different y categories, it can be divided into positive sample subset X^+ and negative sample subset X^- . There is a unit vector $\phi \|\phi = 1\|$ and constant C , which makes (7) true.

$$\begin{cases} \langle X^+ \cdot \phi \rangle < c \\ \langle X^- \cdot \phi \rangle > c \end{cases} \quad (7)$$

For any unit vector ϕ , determine two values

$$\begin{cases} c1(\phi) = \min\langle X^+ \cdot \phi \rangle \\ c2(\phi) = \max\langle X^- \cdot \phi \rangle \end{cases} \quad (8)$$

Find ϕ_0 to maximize the following:

$$r(\phi) = \frac{c1(\phi) - c2(\phi)}{2}, \|\phi\| = 1 \quad (9)$$

The vector ϕ_0 and constant are obtained from the constraint (7) and the maximization function (9)

$$C_0 = \frac{c1(\phi) + c2(\phi)}{2} \quad (10)$$

Determine a hyperplane, distinguish two types of sample sets, and make them have the maximum interval. Refer to formula (9), this hyperplane is called the optimal classification hyperplane, as shown in Fig. 7. It can be seen from the figure that two kinds of linear separable samples are separated by classification lines. The points on the two parallel lines that are cut are the shortest points from the classification lines. The shortest distance is recorded as d , its size is usually positively related to the separation, so that the value d in the optimal classification plane is as large as possible and the segmentation effect is better. The main goal of constructing the optimal hyperplane is found, and a vector and constant B are found to satisfy the following constraints

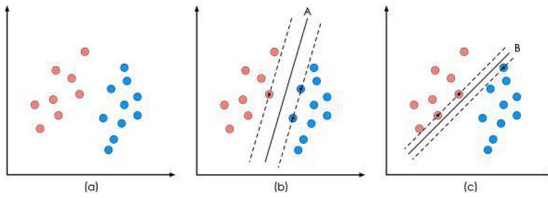


Fig. 7. SVM optimal classification surface.

The main goal of constructing the optimal hyperplane is found a vector W^* and constant b are found to satisfy the following constraints [24].

$$\begin{cases} \langle X^+ \cdot W^* \rangle + b^* \geq 1 \\ \langle X^- \cdot W^* \rangle + b^* \leq -1 \end{cases} \quad (11)$$

And the vector W^* has the minimum norm

$$\min \rho(W) = \frac{1}{2} \|W^*\|^2 \quad (12)$$

$$f(X) = W^* \cdot X + b^* \quad (13)$$

Under the condition of (11), the relationship between the vector obtained by minimization (13) and the vector W^* forming the optimal hyperplane is

$$\phi_0 = \frac{W^*}{\|W^*\|} \quad (14)$$

The interval $r(\phi_0)$ between the optimal hyperplane and the classification vector is

$$r(\phi_0) = \sup \frac{1}{2} (c_1(\phi_0) - c_2(\phi_0)) = \frac{1}{\|W^*\|} \quad (15)$$

In order to find the optimal classification hyperplane, we need to solve the quadratic programming problem. Under the condition of linear constraint (11), we need to minimize the quadratic form, see Eq. (12). It can be solved by Lagrange multiplier method, and the equation is as follows:

$$L(W, a, b) = \frac{1}{2} \|W\|^2 - \sum_{i=1}^N a_i \{y_i \langle X_i \cdot W + b \rangle - 1\} \quad (16)$$

The weight coefficient vector of the optimal classification surface of the support vector, then its optimal classification surface function is:

$$W^* = \sum_{i=0}^N a_i^* y_i X_i \quad (17)$$

The wavelet decomposition method is used to extract the eigenvalues for SVM classification training, and the accuracy reaches 93.72%. Table 1 shows the accuracy after classification training (see Table 1).

Table 1. The accuracy after classification training.

	Motion 1	Motion 2	Motion 3	Motion 4
Motion 1	94	3	0	3
Motion 2	1	93	1	5
Motion 3	1	4	95	0
Motion 4	2	0	4	92

In order to analyze the performance of the algorithm adopted in this paper, the classification accuracy of several feature combinations mentioned in previous literatures is compared. Commonly used feature combinations include time-domain feature combinations: average absolute value (MAV), zero crossing rate (ZC), wavelength (WL), AR model coefficient, and the results are shown in Table 2.

Table 2. The accuracy after classification training.

Feature extraction method	Recognition accuracy
Average absolute value (MAV)	82
Zero crossing rate (ZC)	84
Wave length (WL)	81
AR model coefficient	72

5 Verification

The classification model obtained through training was applied to the lower extremity exoskeleton prototype shown in Fig. 8 to verify the rationality of the conclusions in this paper. According to the indicator light, the subjects made complete continuous movements one by one, each of which was completed 100 times and lasted for 5 s.

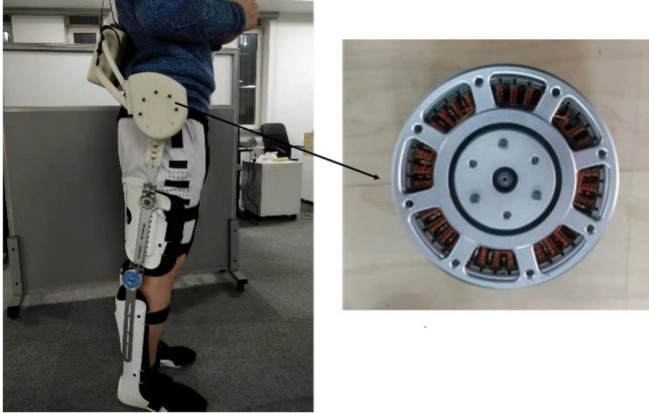


Fig. 8. Lower limb exoskeleton robot prototype.

The classifier model is used for real-time prediction, and the subject controls the exoskeleton to complete the corresponding actions. Figure 9 shows the effect of online real-time exoskeleton movement controlled by a subject. Since it takes some time for the subjects to complete the action according to the change of the indicator light during the experiment, the experimental results will have a slight error and the accuracy will be reduced. After all the subjects completed real-time control of the movement of the lower extremity exoskeleton, the average accuracy of the four groups of continuous movements was 95.14%, 92.51%, 94.30% and 91.78%, respectively. The accuracy statistics results are shown in Fig. 10.

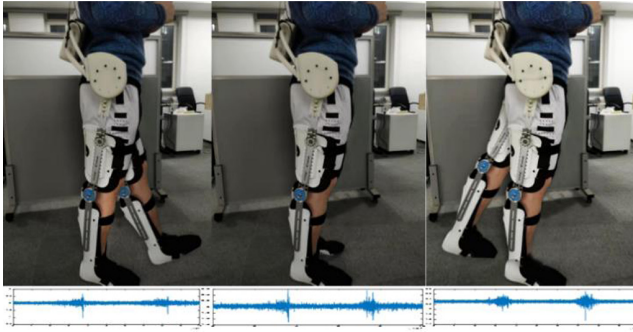


Fig. 9. Real-time control of the exoskeleton movement process.

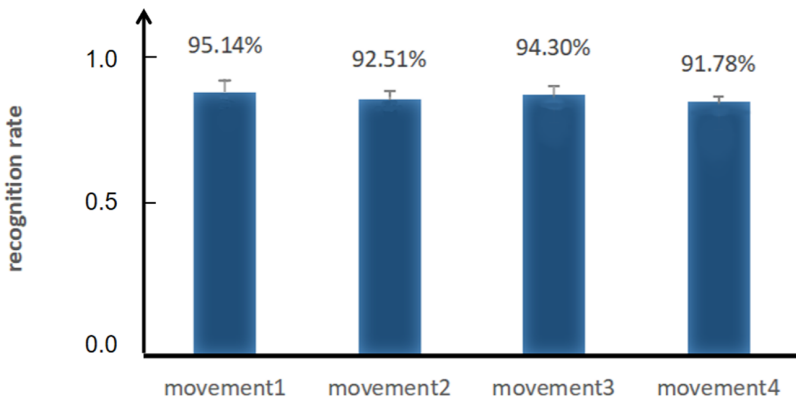


Fig. 10. Four groups of continuous motion accuracy comparison

6 Conclusion

In this paper, a new “time-frequency domain wavelet transform” method is proposed based on the strong temporal sequence of sEMG signal data. The method combines Angle and sEMG to segment the local motion data in the effective leg movement segment as sample data.

At the same time, wavelet analysis is used to extract feature values for parallel support vector machine training, and the Angle classification and recognition of continuous motion are realized. Experimental results show that the preprocessing method and classification recognition algorithm presented in this paper have better classification results. Been method application in the treatment of lower limb exoskeleton robot prototype, lower limb swing to the human body muscle in the process of electrical signals are analyzed in real time, the corresponding relationship between the Angle at the same time, the simulation analysis are carried out using MATLAB, based on the motion process of the lower limbs with multi-channel sEMG analysis, get lower limb joint Angle in the process of sports information, and through the prototype proves the

rationality of the design of lower limb exoskeleton. Through verification experiments, this method is characterized by strong real-time performance and high control accuracy, which shows the application prospect of gait recognition technology based on sEMG signal in the field of exoskeleton, and lays a solid foundation for subsequent research.

Acknowledgements. Liaoning Provincial Department of Education key projects. Research on key technologies for collaborative walking robots based on fine electromyographic signal analysis; Project number: LZGD2019001.

References

1. Zhou, R., Zhuang, R., Huang, C.: Evolution and formation mechanism of population aging pattern in China. *J. Geogr.* **74**(10), 2163–2177 (2019)
2. Song, J.: Evaluation and comparison of nutritional risk of stroke inpatients by different nutritional risk screening tools. *Jilin Univ.* **03**, 64 (2019)
3. Long, Y.: Human motion prediction and human robot coordination control for lower extremity exoskeleton. Harbin Institute of Technology (2017)
4. Millot, P.: Designing human-machine cooperation systems. *J. Phys. Chem. Lett.* **3**(9), 1094–1098 (2016)
5. Zhang, S., Li, X., Zhang, P.: UAV real-time path planning based on human-machine cooperation. *J. Beijing Univ. Aeronaut. Astronaut.* **43**(4), 814–822 (2017)
6. Kamal, S., Jalal, A.: A hybrid feature extraction approach for human detection, tracking and activity recognition using depth sensors. *Arab. J. Sci. Eng.* **41**(3), 1043–1051 (2016). <https://doi.org/10.1007/s13369-015-1955-8>
7. Wei, M.: Research and application of machine learning in trend prediction. Xian University of Technology (2019)
8. Choi, A., Jung, H., Lee, K.Y.: Machine learning approach to predict center of pressure trajectories in a complete gait cycle: a feedforward neural network vs. LSTM network. *Med. Biol. Eng. Comput.* **57**(12), 2693–2703 (2019). <https://doi.org/10.1007/s11517-019-02056-0>
9. Yu, Y.: Ecognition of human lower limb motion and analysis of joint torque based on sEMG signal. Suzhou University (2016)
10. Li, Y., Jin, Z., Ji, S.: Design of a new 3-DOF hybrid mechanical arm. *Sci. China Ser. E: Technol. Sci.* **52**(12), 3592–3600 (2009)
11. Yuan, L., Hu, B., Wei, K.: Control Principle and MATLAB Simulation of Modern Permanent Magnet Synchronous Motor. Beijing University of Aeronautics and Astronautics Press, Beijing (2016)
12. Wang, Z., Zin, H., Zhou, S.: Design and performance analysis of humanoid robot four-DOF manipulator. *Sci. Technol. Vis.* **2020**(09), 137–139 (2020)
13. Liu, X., Li, M.: Effectiveness analysis of muscle fatigue in rehabilitation process based on surface EMG signal. *J. Biomed. Eng.* **36**(01), 6 (2019)
14. Zhang, Y., Jing, Y.: Analysis of descending and mapping of lower extremity surface EMG signals. *J. Sens. Technol.* **31**(07), 1046–1053 (2008)
15. Jiang, Y., Zou, R.: Analysis and recognition of lower limb spasm signal characteristics of surface EMG signals. *Electron. Sci. Technol.* **30**(11), 38–41 (2017)
16. Sun, G., Yan, Z.: Motion classification based on bispectral analysis of surface EMG signals. *J. Beijing Univ. Technol.* **43**(07), 1045–1050 (2017)

17. Liu, J.: Analysis of muscle fatigue based on spectral entropy of multi-channel surface EMG signals. *J. Biomed. Eng.* **33**(03), 431–435 (2016)
18. Shi, W.-T., Lyu, Z.-J., Tang, S.-T.: A bionic hand controlled by hand gesture recognition based on surface EMG signals: a preliminary study. *Biocybern. Biomed. Eng.* **38**(1), 126–135 (2018)
19. Huang, P., Yang, Q.: Feature extraction algorithm of sEMG based on amplitude cube and BP neural network. *China Mech. Eng.* **23**(11), 1332–1336 (2012)
20. Qiao, X., Hu, W.: Sample entropy and wavelet entropy analysis of EEG EMG signal. *J. Test. Technol.* **30**(4), 292–298 (2016)
21. Zou, X., Lei, M.: Pattern recognition of sEMG signal based on multi-scale maximum Lyapunov index. *Chin. J. Biomed. Eng.* **31**(1), 7–12 (2012)
22. Rajagopal, A., Dembia, C.L.: Full-body musculoskeletal model for muscle-driven simulation of human gait. *IEEE Trans. Biomed. Eng.* **63**(10), 2068–2079 (2016)
23. Jie, H., Lu, W.: Hand sEMG recognition based on SVM optimization based on artificial fish swarm algorithm. *Sens. Microsyst.* **35**(02), 23–25 (2016)
24. Lu, L., Liu, S.: Application analysis of sEMG gesture recognition based on nonlinear SVM fusion LDA. *Laser J.* **35**(08), 26–29 (2014)